

Macroporous Polymeric Ion Exchangers as Adsorbents for the Removal of Cationic Dye Basic Blue 9 from Aqueous Solutions

Daniela Suteu,¹ Doina Bilba,¹ Sergiu Coseri²

¹Faculty of Chemical Engineering and Environmental Protection, Gheorghe Asachi Technical University of Iasi, 71A Professor Doctor Docent D. Mangeron Boulevard, Iasi 700050, Romania

²P. Poni Institute of Macromolecular Chemistry of Iasi, 41A Grigore Ghica Voda Alley, 700487 Iasi, Romania

Correspondence to: D. Suteu (E-mail: danasuteu67@yahoo.com)

ABSTRACT: Two macroporous cation-exchange resins, PuroLite C145, a strongly acidic cation macroporous resin, and PuroLite C107E, a weakly acidic cation-exchange resin, were used to remove the dye Basic Blue 9 (BB9) from an aqueous medium. Batch adsorption experiments were carried out to analyze the effect of various parameters, such as the phase contact time, initial dye concentration, initial solution pH, resin dose, and temperature. The experimental equilibrium data were evaluated by the Langmuir, Freundlich, and Dubinin–Radushkevich (DR) adsorption models. The Freundlich model better described the adsorption processes of the BB9 dye onto both cation exchangers, and the monolayer adsorption capacities were established as 31.9846 mg/g (C145) and 27.77 mg/g (C107E) at 20°C. The values of the mean free adsorption energy (E) obtained from the DR model suggested a porous structure of the adsorbents and proposed ion exchange at the main mechanism of the adsorption process. The values of the thermodynamic parameters showed that the retention of the cationic dye was a spontaneous and endothermic process. Environmental scanning electron microscopy and Fourier transform infrared spectroscopy were used to characterize the sorbent and also to validate the adsorption mechanism as ion-exchange ones. The desorption experiments by a batch method were performed with different solutions: 0.1 and 1 mol/L HCl, 2.5 mol/L H₂SO₄, CH₃OH, and a mixture between 1 mol/L HCl and CH₃OH. Desorption performed with sulfuric acid was shown to be most effective because more than 85% of the adsorbed dye was removed. © 2013 Wiley Periodicals, Inc. *J. Appl. Polym. Sci.* 2014, 131, 39620.

KEYWORDS: adsorption; dyes/pigments; resins; separation techniques

Received 7 February 2013; accepted 30 May 2013

DOI: 10.1002/app.39620

INTRODUCTION

Dyes are a class of organic pollutants of aquatic ecosystems coming from the effluents of different industries, such as textiles and leathers, and the production of pharmaceuticals and cosmetics, printing, food, paper, and pulp. Apart from the aesthetic problems related to colored effluents, dyes present in the aquatic environment can reduce light penetration and affect photosynthetic activity and oxygen transfer in the water. Generally, dyes are synthetic chemical compounds with complex aromatic structures, which determine their low degree of biodegradability or even *nonbiodegradability*, their longtime presence in the environment and their accumulation in sediments but especially in fishes or other aquatic organisms. Most dyes are risky substances to living organisms, causing allergies, dermatitis, skin irritation, or different tissular changes. Moreover, aromatic amines, benzidine, naphthalene, and other aromatic compounds that result as byproducts of azo dye degradation by microorganisms have been reported to be toxic, carcinogenic, and mutagenic to humans.¹

To minimize environmental damage, in most countries, stricter laws and regulations have been introduced, and more stringent standard discharge limits of colored industrial effluents have imposed a decolorization step in wastewater treatment plants. Therefore, the removal of dyes from industrial effluents before their discharge into aquatic ecosystems is of considerable concern.

There are a variety of treatment technologies for colored wastewater, including chemical oxidation, coagulation/flocculation, ozonation, ion exchange, adsorption, electrochemical reduction, membrane processes, and biological degradation; the advantages and limitations of each method have been highlighted by different authors.^{2–5}

Adsorption onto various materials is one of the methods that is very useful in the treatment of wastewater containing dyes. In the adsorption process, a soluble chemical species (an *adsorbate*) is removed from the liquid phase by attachment to the surface

Table I. Application of Ion-Exchange Resins as Adsorbents for the Removal of Different Dyes

Ion exchange resins used and their main characteristics	Removed dye	Reference
Gel anion exchangers (weakly basic Amberlite IRA-67 and strongly basic Amberlite IRA-458)	Acid Orange 7	6
Strongly basic polystyrene anion exchangers: Amberlite IRA-900 and Amberlite IRA-910	Tartrazine	7
Acrylic resins: Amberlite IRA-458 with a gel structure and Amberlite IRA-958 with a macroporous structure	Reactive Black 5	8
Gel anion exchanger Purolite A-850 of N ⁺ (CH ₃) ₃ functional groups	Acid Blue 29	9
Strongly basic anion exchanger of macroporous structure: Purolite A-520E	Acid Blue 29	10
Purolite ion-exchange resins of the macroporous (A-500) and gel (A-400) structures	Blue M-EB reactive dye	11
Strong cation-exchange resin obtained by poly(glycidyl methacrylate) grafted via surface-initiated atom transfer radical polymerization on a crosslinked acrylate-based resin	Crystal Violet and Basic Fuchsin	12
Acrylic weak base anion-exchange resin with ethylenediamine functional groups	Acid Green 9	13
Polystyrene anion exchangers Amerlite IRA-900 and Amberlite IRA-910 with a macroporous structure	Allura Red and Sunset Yellow	14
Weakly basic anion exchange resins of phenol-formaldehyde (Amberlyst A 23), polyacrylate (Amberlite IRA 67) and polystyrene (Lewatit MonoPlus MP 62) matrices	Remazol Black - reactive dye	15
Weak base macroporous Anion Exchanger Amberlite FPA51	Acid Blue 74	16
Polystyrene anion exchangers Amerlite IRA-900 and Amberlite IRA-910 with macroporous structure		
p(VBC) (cross-linked poly(vinyl benzylchloride) — COOH beads	Methylene Blue and Crystal Violet	17

of an insoluble rigid particle (an *adsorbent*) via physical and/or chemical bonds. Adsorption is recognized as an attractive method for dye removal from wastewater because of the specific physicochemical interactions between dyes and the solid adsorbent; its design simplicity, flexibility, and insensitivity to toxic substances; its low cost; its low matrix effect; and the possibility of using a broad variety of materials as adsorbents. The selection of the adsorbent is based on requirements concerning high selectivity, large capacity of adsorption, favorable kinetic features, physicochemical stability, mechanical strength, easy regeneration, and availability at low cost. Taking into consideration these aspects, we can delineate two classes of adsorbents:

1. Synthetically prepared materials, such as activated carbon, ion-exchange resins, polyamide, ion-exchange celluloses, and functionalized polymers.^{1,18}
2. Unconventional low-cost materials, including a large number of natural materials (clays, e.g., sepiolite, montmorillonite, and bentonite; chitosan; peat; cotton; hemp fibers; biomass) or the wastes/byproducts of agricultural and industrial processes (bagasse pith, maize cob, rice husk, coconut shell, sawdust, fly ash, metal hydroxide sludge, etc.), which can be used as they are or after a minor treatment.

Commercially available activated carbon has been widely used in the wastewater treatment of colored wastewater,^{19,20} but because of their high cost, recent research has focused on the development of alternative low-cost adsorbents.^{21–25}

Even so, the scientific literature contains some valuable information about the applicability of ion-exchange resins in the removal of dyes from aqueous solutions, probably because of their advantages related to ease of use in dynamic systems with increased adsorption efficiency, the possibility of using them in several consecutive adsorption–desorption cycles, and their high performance in terms of degree of discoloration and treatment of aqueous effluents.^{26–28} The major advantages outweigh the high cost of the synthetic resins involved.

Various ion-exchange resins (commercially or synthesized by authors) investigated recently for the removal of dyes from aqueous solutions are summarized in Table I.

The related literature does not mention more than few studies on the removal of cationic dyes, although they are more toxic and harmful than anionic dyes.

The aim of this research was to study the efficiency of two commercially available macroporous cation-exchange resins, Purolite

Table II. Physicochemical Characteristics of the Purolite Cation-Exchange Resins

Characteristic	C145	C107E
Polymer matrix structure	Macroporous polystyrene crosslinked with divinylbenzene	Macroporous polymethacrylic crosslinked with divinylbenzene
Functional group	Sulfonic acid ($-\text{SO}_3^-$)	Carboxylic acid ($-\text{COO}^-$)
Ionic form, as shipped	Na^+	H^+
Typical mean size (mm)	0.60–0.85	0.60–0.85
Moisture retention (%)	55–60	53–58
Shipping weight (g/L)	770–805	700–730
Operating pH range	0–14	5–14
Maximum operating temperature	140°C	100°C
Total exchange capacity (equiv/L, equiv/kg of dry resin) ^a	1.5, 4.55	3.7, 9.4

^aDetermined by the pH metric titration of resins dried at room temperature for 72 h.

C145 (a strong acid) and Purolite C107E (a weak acid), in the removal Basic Blue 9 (BB9) dye, which was selected as typical basic textile dye, from aqueous solutions. The adsorption behavior of the cationic resins was evaluated by the determination of the effect of some experimental parameters (i.e., the initial dye concentration, solution pH, adsorbent dose, phase contact time, and temperature) on the dye removal and by the study of the adsorption isotherms and thermodynamics of the adsorption process. To obtain more information about the adsorption mechanism, scanning electron microscopy and Fourier transform infrared (FTIR) spectroscopy were used.

EXPERIMENTAL

Characterization of the Ion-Exchange Resins

The experiments were carried out with two types of commercially available cation-exchange resins provided from Purolite International, Ltd. (United Kingdom); their characteristic properties from the guidelines of the manufacturer are listed in Table II.

Dye Solution

BB9 is a synthetic dye that is extensively used in the printing and textile industries, as an additive in formulations of different drugs in the pharmaceutical industry, in the medical field for its antimalarial activity, as a component of disinfection solutions,²⁹ and as a redox indicator. It is not considered an acutely toxic dye, but excess amounts and short periods of exposure have many harmful effects on living organisms.³⁰ Although it is not strongly hazardous, this dye is usually used as a model basic dye in studies concerning techniques for textile wastewater decolorization.¹¹ The BB9 dye (CI 52015, Standard Fluka AG) was used without further purification as a commercial salt. The dye is structurally (Figure 1) a heterocyclic aromatic compound (a phenothiazine dye) with the molecular formula $\text{C}_{16}\text{H}_{18}\text{N}_3\text{S}\text{Cl}$, molecular weight of 319.85 g/mol, and maximum wavelength of 660 nm. It is present in ionic form with chloride as the exchangeable ion. An aqueous stock solution of 320 mg/L was prepared by dissolution of the corresponding amount of dye in double-distilled water; all working solutions were prepared by appropriate dilutions.

Adsorption Method and Methodology

The dye adsorption experiments were carried out by a batch technique. Samples of the dried cationic resins accurately weighed into the conical flasks (150 mL) were put in contact with 25-mL aqueous solutions containing known concentrations of dye. The flasks were kept in a thermostatic bath (Poleko SLW 53) at a selected constant temperature with intermittent shaking until it reached equilibrium (5 h). The dye concentration in the supernatant was determined spectrophotometrically. The efficiency of the dye removal was evaluated by means of the percentage of dye removal [R (%); eq. (1)] and by the amount of retained dye [q ; mg of dye/g of dry resin; eq. (2)]:

$$R = \frac{(C_0 - C)}{C_0} \cdot 100 \quad (1)$$

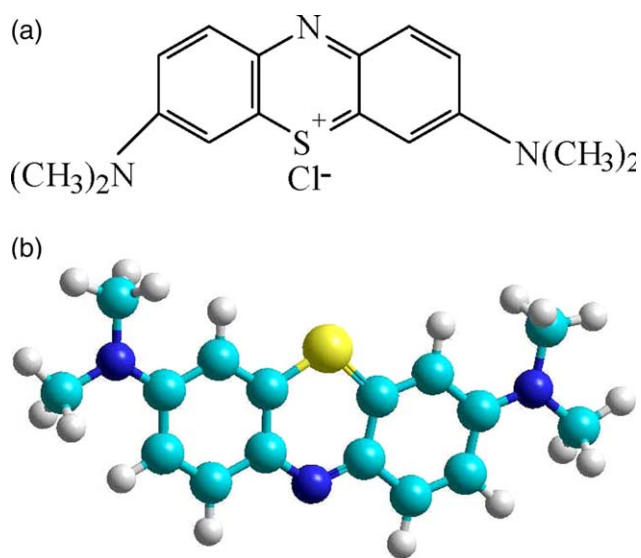


Figure 1. Chemical and molecular structure of the BB9 dye. [Color figure can be viewed in the online issue, which is available at wileyonlinelibrary.com.]

$$q = \frac{(C_0 - C)}{G} \cdot V \quad (2)$$

where C_0 and C are the initial and the equilibrium (residual) concentration of the dye in solution (mg/L), G is the amount of dry resin (g), and V is the volume of solution (L).

Data Evaluation

To test the best fitting isotherm models for the experimental data, we used the classical linear regression analyses on basis of the value of the correlation coefficient (R^2), and also newer methods such as the χ^2 statistic test [eq. (3)]³¹ and the residual root mean square error [RMSE; eq. (4)].³² Small values of the χ^2 test and RMSE indicate a better correlation between the experimental and calculated data of the adsorption capacity, and also indicate acceptable experimental errors.³¹

$$\chi^2 = \sum_{i=1}^N \frac{(q_{e,\text{exp}} - q_{e,\text{calc}})^2}{q_{e,\text{calc}}} \quad (3)$$

$$\text{RMSE} = \sqrt{\frac{1}{N-2} \sum_{i=1}^N (q_{e,\text{exp}} - q_{e,\text{calc}})^2} \quad (4)$$

where $q_{e,\text{exp}}$ and $q_{e,\text{calc}}$ are the experimental and calculated values of the adsorption capacity and N is the number of experimental data.

Analytical Methods for Quantitative Determinations and Physicochemical Characterization

The residual concentrations of BB9 dye in aqueous samples were determined spectrophotometrically by measurement of the absorbance at a maximum dye wavelength of 660 nm with a JK-VS-721N VIS spectrophotometer and interpolation with a calibration curve (the working concentration range in the Lambert–Beer region was 1.3–5.1 mg/L).

The solution pH was measured with a Radelkis OP-271 pH/ion analyzer.

FTIR Spectroscopy. The FTIR spectra for the copolymer, the studied dye, and the dye attached to the copolymer microbeads were obtained with a Bruker Vertex 70 instrument. All the spectra were the results of 256 co-added scans at a resolution of 4 cm^{-1} in KBr pills in the working range 400–4000 cm^{-1} .

Environmental Scanning Electron Microscopy (ESEM). The structural characterization of the copolymer microbeads before and after dye attachment was performed by ESEM. The ESEM studies were performed on a Quanta 200 instrument. The samples were fixed by means of colloidal silver on copper supports. The samples were covered with a thin layer of gold by sputtering (EMITECH K 550x). The coated surface was examined with the Quanta 200 operating at 5 kV with secondary electrons in high-vacuum mode.

Desorption and Regeneration Studies

The dye desorption experiments were also carried out by a batch technique. Samples of 0.2 g of dried resin loaded with BB9 were equilibrated into conical flasks (150 mL) with 25-mL solution of various reagents used for desorption: 0.1 and 1M HCl, 2.5M

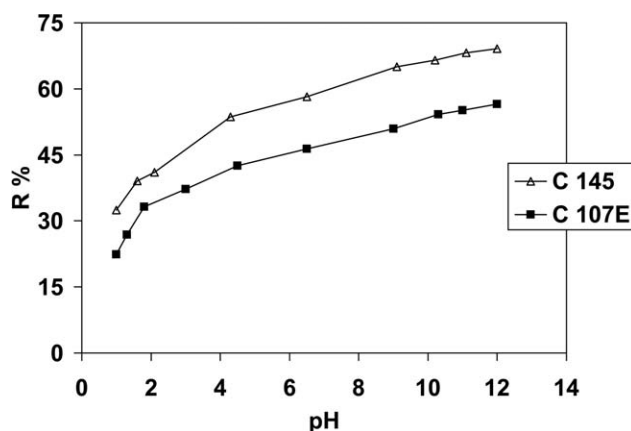


Figure 2. Effect of the solution pH on the BB9 dye adsorption onto Puro-lite cation-exchange resins. Conditions: 10 g of resin/L, initial concentration = 51.2 mg of dye/L, and temperature = 20°C.

H_2SO_4 methanol, and a 1M HCl/methanol (1:1) mixture. The flasks were kept in a thermostatic bath (Poleko SLW 53) at a 20°C constant temperature with intermittent shaking for a determined time (4 and 24 h). At the end of the experiment, the mixtures were filtered, and 2 mL of the filtrate was collected for spectrophotometric analysis of the desorbed dye. The efficiency of the dye desorption was evaluated by means of the amount of desorbed dye (q_{des} ; mg of dye/g of resin)⁻¹ [eq. (5)] and by the percentage of dye desorbed [R_{des} ; %; eq. (6)]:

$$q_{\text{des}} = C_{\text{des}} \frac{V}{g} \quad (5)$$

$$R_{\text{des}} = \frac{q_{\text{des}}}{q} \cdot 100 \quad (6)$$

where C_{des} is the concentration of dye desorbed in solution (mg/L), V is the volume of eluent (L), and g is the amount of resin loaded with dye (g).

The recovered resins were washed with distilled water several times and then reused in several cycle adsorption–desorption experiments.

RESULTS AND DISCUSSION

Effect of the Solution pH

The solution pH is one of the most important experimental factors that adjust the ion-exchange selectivity in the adsorption process on ion-exchange resins. The pH value determines the specific adsorbent surface charge, the ionic dissociation of dye in solution, and at the same time, the distribution of ionized species between phases. This physical parameter is most important in the case of weakly acidic resins because it affects the degree of protonation and dissociation of the functional groups.

To study the effect of the initial pH of the dye solution on the adsorption of BB9 dye onto both ion exchangers, samples of 0.4 g of the resins were put in contact with 25-mL volumes of dye solution with initial concentrations of 51.2 mg of dye/L. The solution pH was adjusted to the required value with 1N HCl and NaOH solutions. The entire assembly was maintained at 20°C with intermittent stirring until it reached the established equilibrium time (5 h), and then we determined spectrophotometrically the dye concentration in the supernatant. Figure 2

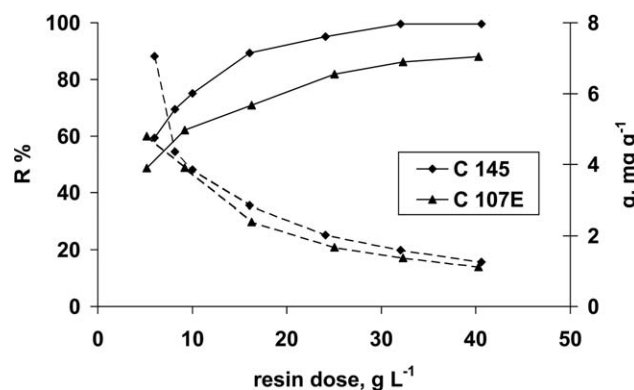


Figure 3. Effect of the resin dose on the adsorption of the BB9 dye. Conditions: initial dye concentration = 51.2 mg/L, temperature = 20°C, pH 10, contact time = 5 h. (---) q (mg/g) and (—) R (%).

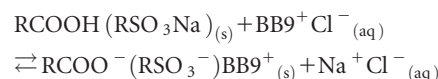
shows the relationship between the pH value and the removal of BB9 dye.

As shown in Figure 2, as the solution pH increased, R increased for both cationic resins. The lowest values of removal efficiency were obtained in acidic solutions (pH = 1–3). Although the behavior of the two resins was similar, the explanations were different. The sulfonic groups of the strongly acidic C145 resin were highly ionized and suitable for the dye cation removal over the entire solution pH range; the decrease in dye removal at pH < 2 may have been due to the higher concentration of protons (H^+) which competed with the cationic dye molecules for interaction with active sites ($-SO_3^-$ groups) of the resin. After that, the strongly acidic functional groups of the C145 PuroLite resin were less affected by pH variation, and the removal capacity of the resin slightly increased with increasing pH. The weakly acidic carboxylic groups of the C107E resin were completely protonated at low pH values (<2) and were unable to form electrostatic interactions with the cationic dye. Increasing the solution pH increased the dissociation of the $-COOH$ groups and enlarged the attraction between the cationic dye and the sorbent surface; at pH = $pK_a = 3.6$, the dissociation degree was 0.5, and complete dissociation occurred at pH > 5.6. Also, a further increase in pH slightly increased the removal efficiency of the cationic resins, and in alkaline media and for both resins, the removal percentage had maximum values. Similar observations were obtained by other authors.^{10,33} To prevent the aggregation of the BB9 molecules in solution with pH values above 10, the following experiments were carried out at pH 10.³⁴

However, an important amount of dye was adsorbed on the weakly acidic PuroLite C107E at low pH values when the carboxylic groups were protonated so that the electrostatic interaction between the negative charge of the resin and the positive charge of the dye molecules could not be considered the unique mechanism of the adsorption. This suggested that other interactions contributed to the binding of dye molecule on the resin surface, most probably hydrogen bonding between the $-OH$ of the carboxyl groups as hydrogen donors and the nitrogen atoms from BB9 dye as hydrogen acceptors. As shown in Figure 2, the removal efficiency of the sulfonic resin C145 was slightly higher

than of the carboxylic resin C107E; this behavior may have been due to the existence of the secondary hydrophobic interactions between the aromatic rings of the polystyrene matrix (C145) and the conjugated structure ($-N=C-C=C-$) of the BB9 dye.

These explanations were in accordance with the literature data³⁵ and on their basis might reveal that the dye retention could be described by the following relation:



Effect of the Resin Dose

The effect of the amount of resin on the cationic dye adsorption was examined with amounts of resins between 0.1 and 1.5 g. These were equilibrated at 20°C with 25-mL volumes of dye solution with initial concentration of 51.2 mg of dye/L (pH 10) under conditions of intermittent stirring. After the equilibrium time was attained, we analyzed the aqueous phases. The results are presented in Figure 3.

The results from Figure 3 show that with increasing resin dose from 4 to 40 g/L, R increased from 55.937 to 99.533% for the C145 resin and from 48.7 to 88% for C107E. At the same time, increasing the resin dose decreased the amount of cationic dye retained per unit weight of dry resin (from 7.06 to 1.255 mg/g for the C145 resin and from 4.795 to 1.118 mg/g for the C107E resin). This behavior could be explained by the fact that the increase in the resin amount determined the increase in the number of available adsorption sites (and increased the R values), but some of these sites remained unsaturated during the adsorption process (which decreased the q values). Similar results were reported by Noor and Al-Solmi.³⁶ The differences between the removal efficiency of the studied cation-exchange resins may have been due to their different hydrophobic characteristics (which were weaker for the polyacrylic resin).

Effect of the Contact Time

The experimental data showed that the retained amounts of the dye increased with increasing phase contact time. The adsorption rate was fast in the beginning of the contact time and then decreased gradually until the adsorption process reached equilibrium. For both resins and a solution with a 51.2 mg/L initial dye concentration, the time necessary to achieve the equilibrium was about 5 h. After that time, the amount of dye adsorbed increased very little by only 2–3%.

Effect of the Initial Dye Concentration and Temperature

The effect of the initial dye concentration on the BB9 dye adsorption onto the PuroLite cationic resins was investigated with an adsorbent dose of 10 g/L; the adsorbent was in contact with 25-mL aqueous solutions containing dye solution with concentrations in the range 12.8–239 mg/L (pH 10). The flasks were kept in a thermostatic bath (Poleko SLW 53) at a constant temperature of 5, 20, or 50°C with intermittent shaking until equilibrium was reached; then, the aqueous phases were analyzed to establish the residual dye content. The results are presented in Table III.

The results from Table III show that for both resins, the percentage of dye removed at a constant temperature decreased

Table III. Effects of the Initial Dye Concentration and Temperature on the BB9 Dye Adsorption onto Purolite C145 and Purolite C107E Cation-Exchange Resins

Cationic resin	Initial dye concentration (mg/L)	5°C		20°C		50°C	
		q (mg/g)	R (%)	q (mg/g)	R (%)	q (mg/g)	R (%)
C145	29.6	2.77	93.58	2.84	95.945	2.9	97.973
	51.2	4.71	91.99	4.9	95.703	5.01	97.85
	123.2	11.1	90.097	11.55	93.75	12	97.565
	192	16.7	86.98	17.8	92.708	18.6	96.875
C107E	29.6	2.71	91.554	2.825	95.44	2.89	97.635
	51.2	4.6	89.84	4.84	94.53	4.98	97.265
	123.2	10.8	87.66	17.50	92.614	18.45	96.75
	192	16.2	84.38	21.20	91.146	24.92	96.094

pH 10, 10 g of resin/L, contact time = 5 h.

with increasing initial dye concentration. At the same time, at a constant dye concentration, the removal percentage of cationic dye increased with increasing temperature. So, the highest value of removal efficiency (98%) was obtained in diluted solutions of the dye (29.6 mg/L) at a temperature of 50°C with the strongly acidic cationic resin C145 and the lowest (84.4%) in solutions with 192 mg of dye/g at 5°C with the weakly acidic resin C107E. The effect of the dye concentration was more important at a temperature of 5°C (an increase in the initial dye concentration from 29.6 to 192 mg/L decreased the dye removal efficiency by 6–7%) and was at a minimum at 50°C (in the same concentration range, the removal efficiency decreased by 1–1.5%).

Adsorption Isotherms

The adsorption isotherm describes the distribution at equilibrium of the adsorbed species between the liquid phase and the solid phase at a constant temperature, and this distribution was represented graphically by means of the function $q = f(C)$, where q represents the amount of dye retained per unit weight of dry resin (mg/g) and C is the equilibrium concentration of dye in solution (mg/L). The analysis of the adsorption isotherms is useful in obtaining valuable information about the adsorption mechanism, the adsorbent surface properties and affinities, for the design of adsorption systems. The adsorption isotherms of BB9 dye on the two types of Purolite cationic resins measured at three temperatures, 2, 20, and 50°C, are presented in Figure 4.

To establish the most appropriate correlations for the equilibrium curves, the adsorption isotherms of BB9 dye on the studied Purolite cation-exchange resins were investigated with three of the well-known isotherm models, that is, the Freundlich, Langmuir, and Dubinin–Radushkevich (DR) models, as expressed by following equations:³⁷

$$q = K_F \cdot C^{1/n} \quad (7)$$

$$q = \frac{K_L \cdot C \cdot q_0}{1 + K_L \cdot C} \quad (8)$$

$$\ln q = \ln q_0 - B\varepsilon^2; \varepsilon = rT \ln \left(1 + \frac{1}{C}\right); E = \frac{1}{\sqrt{2B}} \quad (9)$$

where K_F and $1/n$ are Freundlich constants related to the adsorption capacity and adsorption intensity (efficiency), respectively; q_0 is the maximum amount of adsorbed dye (mg/g); K_L is the Langmuir constant related to the binding energy of the solute (L/mg); B is the activity coefficient related to the mean free adsorption energy ($\text{mol}^2 \text{kJ}^2$), ε is the Polanyi potential, r is the universal gas constant (8.314 J/mol K), and E is the mean free adsorption energy (kJ/mol).

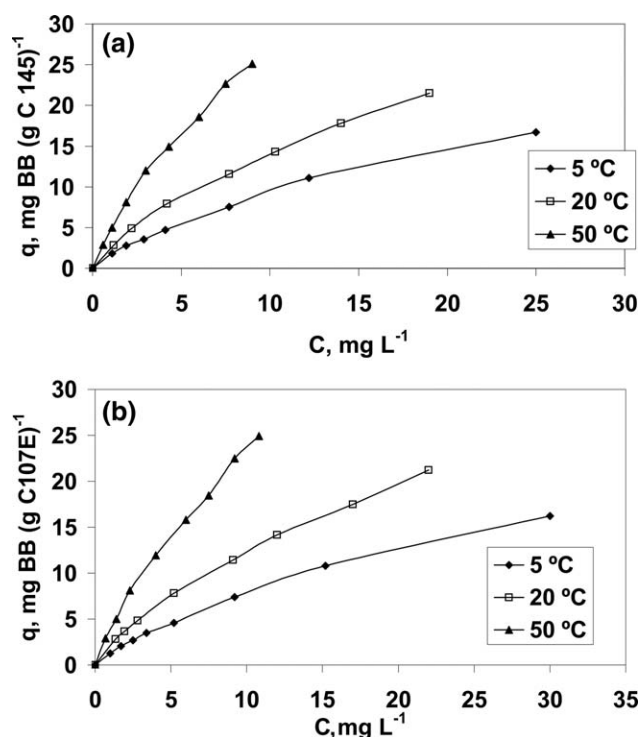


Figure 4. Adsorption isotherms of the BB9 dye (BB) on the Purolite cationic resins: (a) C145 and (b) C107. Conditions: pH 10; 10 g of resin/L, contact time = 5 h.

Table IV. Isotherm Constants for the Adsorption of the BB9 Dye onto Purolite Resins

Isotherm models	Purolite C145			Purolite C107E		
	5°C	20°C	50°C	5°C	20°C	50°C
Freundlich						
K_F [(mg/g)(L/mg) ^{1/n}]	1.70 ± 0.048	2.65 ± 0.097	4.63 ± 0.139	1.35 ± 0.0378	2.288 ± 0.034	3.922 ± 0.0912
n	1.38 ± 0.029	1.386 ± 0.044	1.264 ± 0.034	1.335 ± 0.026	1.379 ± 0.014	1.277 ± 0.023
R^2	0.9978	0.9968	0.9957	0.9977	0.9994	0.998
RMSE	0.493	0.2504	0.394	0.477	0.393	0.712
χ^2	0.108	0.0269	0.077	0.088	0.068	0.196
Langmuir						
q (mg/g)	21.831 ± 5.439	31.9846 ± 2.529	50.989 ± 2.175	17.46 ± 2.601	27.77 ± 6.160	41.768 ± 5.673
K_L (L/mg)	0.0726 ± 0.004	0.0811 ± 0.0012	0.1002 ± 0.001	0.078 ± 0.0019	0.0807 ± 0.0025	0.106 ± 0.0024
R_L	0.418 ± 0.067	0.294 ± 0.06	0.252 ± 0.037	0.48 ± 0.063	0.295 ± 0.05	0.245 ± 0.036
R^2	0.9856	0.9989	0.9998	0.9963	0.994	0.9968
RMSE	1.722	1.556	1.435	1.401	1.069	0.574
χ^2	1.195	0.749	0.541	0.529	0.3005	0.093
DR						
q_0 (mg/g)	313.822 ± 29.79	460.769 ± 23.65	1024.691 ± 73.21	308.104 ± 16.41	432.44 ± 15.57	877.98 ± 58.45
B (mol ² /kJ)	0.0063	0.0055	0.0047	0.0065	0.0056	0.0047
E (kJ/mol)	8.923 ± 0.1015	9.578 ± 0.0625	10.358 ± 0.0806	8.75 ± 0.54	9.483 ± 0.043	10.336 ± 0.077
R^2	0.9974	0.9992	0.9985	0.9986	0.9995	0.9986
RMSE	0.185	0.201	0.398	0.299	0.195	0.425
χ^2	0.0273	0.0166	0.062	0.0563	0.0225	0.0716

Table V. Thermodynamic Parameters of the BB9 Dye Adsorption onto the Purolite Resins as Calculated with K_0

C_0 (mg/L)	T (K)	Purolite C145						Purolite C107E				
		K_0	T_0 (K)	ΔG^0 (kJ/mol)	ΔH^0 (kJ/mol)	ΔS^0 (J mol ⁻¹ K ⁻¹)	K_0	T_0 (K)	ΔG^0 (kJ/mol)	ΔH^0 (kJ/mol)	ΔS^0 (J mol ⁻¹ K ⁻¹)	
29.6	278	14.58	211.19	-6.193	19.759	93.508	10.84	220.66	-5.508	21.712	98.479	
	293	23.67		-7.707			20.93		-7.407			
	323	48.33		-10.414			41.29		-9.991			
51.2	278	11.49	221.01	-5.642	22.407	101.43	8.846	226.27	-5.039	22.635	100.08	
	293	22.27		-7.559			17.29		-6.942			
	323	45.55		-10.254			35.57		-9.591			
123.2	278	9.098	230.93	-5.103	24.724	107.14	7.105	232.91	-4.532	23.669	101.58	
	293	15.0		-6.597			12.54		-6.160			
	323	40.07		-9.911			29.8		-9.116			
192	278	6.68	236.12	-4.389	25.238	106.84	5.4	239.6	-3.898	24.905	103.91	
	293	12.71		-6.194			10.29		-5.680			
	323	31.0		-9.222			24.6		-8.600			

The characteristic parameters of each isotherm model calculated from the intercepts and slopes of the corresponding linear plots ($\log q$ vs $\log C$, $1/q$ vs $1/C$, and $\ln q$ vs ε^2 ; figures not shown) are presented in Table IV. The applicability of these models was evaluated with their uncertainties (standard deviation) and values of R^2 , residual RMSE, and χ^2 test (Table IV).

The R^2 values showed that both the Freundlich isotherm model (multilayer adsorption onto a heterogeneous surface with different adsorption sites) and the Langmuir model (the maximum adsorption corresponded to a monolayer of dye molecules on the adsorbent surface containing a finite number of energetically equivalent sites) described the adsorption of the dye onto both Purolite resins well. However, a comparison of the values of the residual RMSE and χ^2 test (Table IV) suggested that the experimental data of cationic dye adsorption by both ion-exchange resins were more appropriate to the Freundlich isotherm model. This behavior may be in agreement with the aggregation tendency of the BB9 dye, especially at higher concentrations, and with the possibility of uptake of the dye through many types of interactions. The values of the Freundlich parameter K_F increased with increasing temperature; this suggested that the adsorption of the cationic dye onto the studied Purolite resins was favored at high temperatures. In all cases, the value of n is greater than unity and indicated good adsorption of dye.

The Langmuir constants q_0 , which reveals the accessibility of adsorption sites, and K_L , which reflects the binding energy between the dye molecules and functional groups from the surface of the ion-exchange resins, increased with increasing temperature; this suggested that the adsorption could be an endothermic process.

The essential features of the Langmuir isotherm could be expressed by means of the dimensionless constant R_L (which is a separation factor or equilibrium parameter) as calculated by the following equation:³⁸

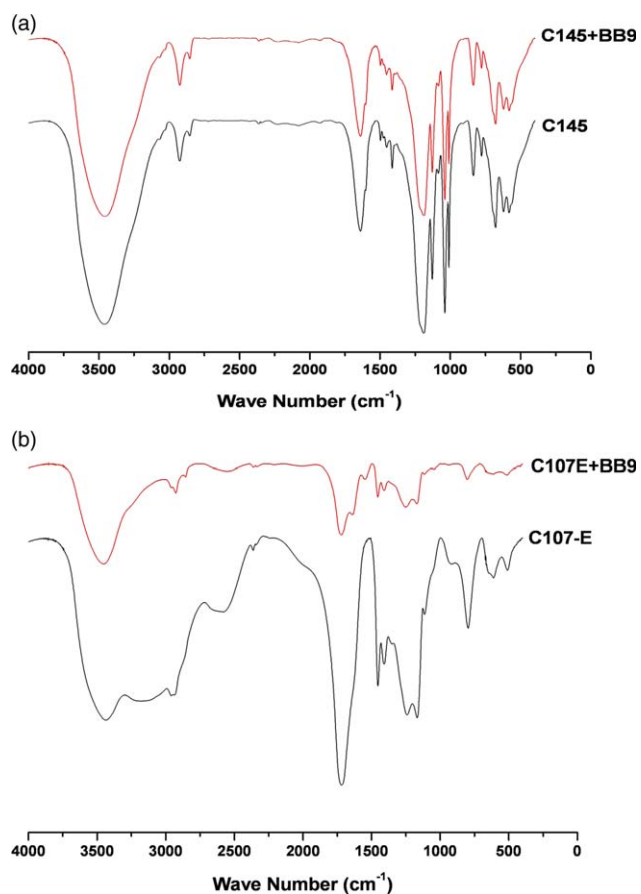


Figure 5. FTIR spectra of the (a) C145 resin before and after dye adsorption and (b) C107E resin before and after dye adsorption. [Color figure can be viewed in the online issue, which is available at wileyonlinelibrary.com.]

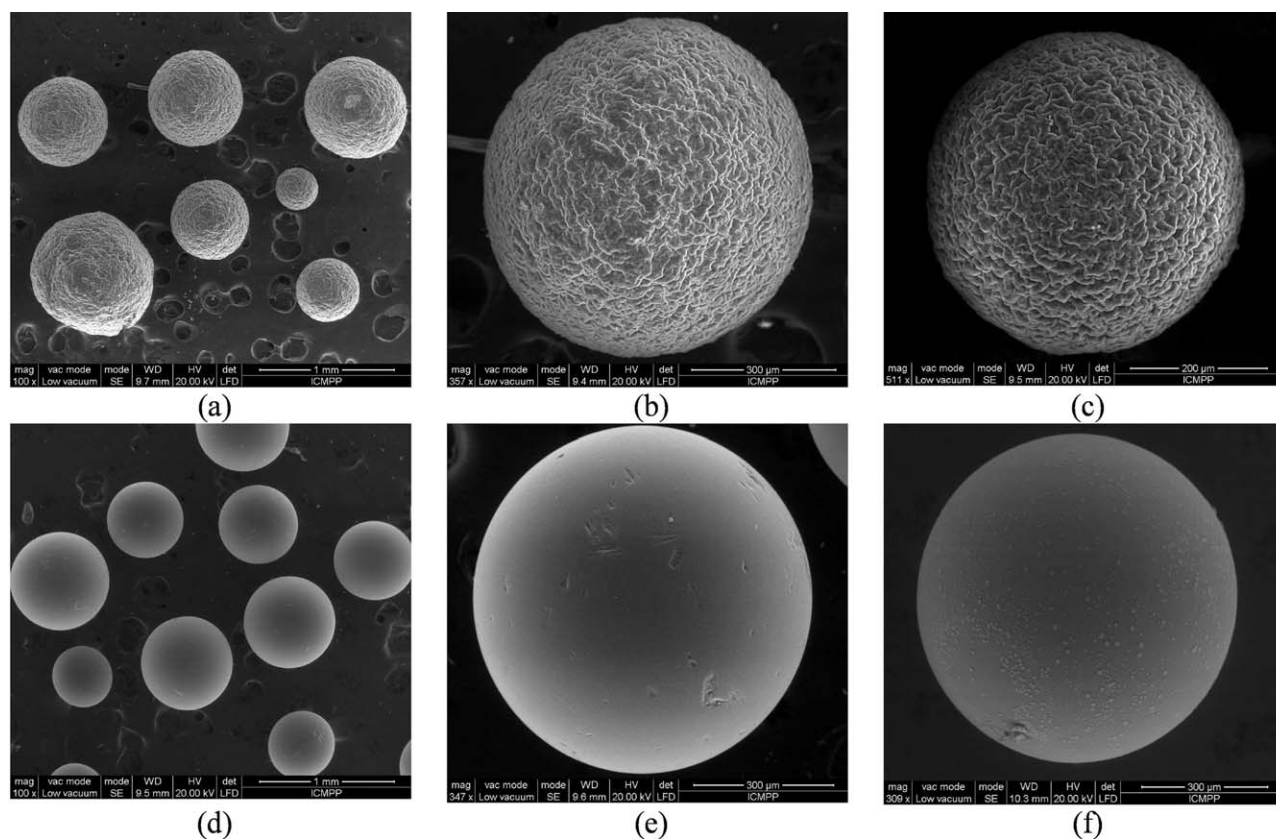


Figure 6. ESEM images for (a,b) C107E, (c) C107E-MB, (d,e) C145, and (f) C145-MB.

$$R_L = \frac{1}{1 + K_L \cdot C_0} \quad (10)$$

The value of R_L indicates the shape of the isotherms to be either unfavorable ($R_L > 1$), linear ($R_L = 1$), favorable ($0 < R_L < 1$), or irreversible ($R_L = 0$). The values of R_L were in the range 0–1 (Table IV); this confirmed the favorable adsorption of BB9 dye onto both cationic resins.

The values of E calculated by the DR equation (Table IV) showed that at all three temperatures for both resins ($E_{C145} = 8.909$ – 10.314 kJ/mol, $E_{C107E} = 8.7706$ – 10.314 kJ/mol), the values were characteristic for an ion-exchange mechanism of dye adsorption by cationic resins.

The adsorption capacity in the DR equation (q_0), which may represent the total specific mesopore and macropore volume of the adsorbent, was found to be much higher than the q value obtained with the Langmuir isotherm model for both resins and at all three temperatures. These could be explained by the existence of a porous structure in the adsorbent. Similar results have been reported in the literature for other materials as adsorbents but not yet for ion-exchange resins.

Thermodynamic Studies

To obtain more information about the mechanism of cationic dye adsorption onto the studied Purolite resins and to predict the feasibility of the adsorption process, some characteristic

Table VI. Results of the Desorption Study of the BB9 Dye from Purolite C145 and C107E Resin Ion Exchangers

Desorption conditions	C145			C107E			
	q (mg/g)	q^{des} (mg/g)	R (%)	q (mg/g)	q^{des} (mg/g)	R (%)	
0.5M HCl, 24 h	22.405	0.904	4.03	22.21	3.29	14.81	
1M HCl, 24 h	17.026	0.358	2.1	17.975	5.696	31.69	
CH ³ OH, 24 h	19.78	0.479	2.42	20.284	0.682	3.36	
1M HCl: CH ³ OH (1:1), 24 h	19.78	2.72	13.75	20.284	11.55	56.94	
H ² SO ⁴ 2.5M	24 h, 20°C	18.97	16.74	88.24	19.44	18.46	94.96
	4 h, 20°C	18.87	10.92	57.87	19.44	14.54	74.79
	4 h, 50°C	22.63	14.48	63.98	19.76	17.34	87.74

thermodynamic parameters, such as the free-energy change (ΔG^0), enthalpy change (ΔH^0), and entropy change (ΔS^0), were calculated with eqs. (9) and (10):³⁷

$$\Delta G^0 = -rT \ln K \quad (11)$$

$$\ln K_0 = -\frac{\Delta H^0}{r \cdot T} + \frac{\Delta S^0}{R} \quad (12)$$

where T is the temperature (Kelvin), r is the universal gas constant ($8.314 \text{ J mol}^{-1} \text{ K}^{-1}$).

Literature data indicate different methods for evaluating the equilibrium constant (K_0).^{39,40} In our study, K_0 was considered a dimensionless parameter, and it was calculated with eq. (13)⁴⁰ (Table V):

$$K_0 = \frac{C_s}{C_l} \quad (13)$$

where C_s is the solid-phase dye concentration at equilibrium (mg/L) and C_l is the liquid-phase dye concentration (mg/L).

The values of the thermodynamic parameters obtained with eqs. (9) and (10), the linear dependence $\ln K$ versus $1/T$ (not presented in this article), and R^2 are given in Table V.

The negative values of ΔG^0 obtained for both resins indicated that the adsorption process of the selected dye was always a thermodynamically feasible and spontaneous process. The positive values of ΔH^0 obtained suggested the endothermic nature of the adsorption process of BB9 cationic dye onto the studied resins, and the positive value of ΔS^0 showed that the spontaneity of the adsorption process was assured only under conditions when $\Delta H^0 < T\Delta S^0$.

For further technological approaches, it is of great interest to know the optimum temperature at which the adsorption process is the most feasible and spontaneous. The zero standard free-energy temperature (T_0) represents the temperature at which the standard free energy is zero and can be evaluated from eq. (12) under conditions of $\Delta G^0 = 0$.³⁹ The value of this parameter can be graphically determined as the intercept ($\Delta G^0 = 0$) of the vertical axis with a graphical representation of the variation of standard $\Delta G^0 T$:

$$\Delta G^0 = \Delta H^0 - T\Delta S^0, T_0 = \Delta H^0 / \Delta S^0 \quad (14)$$

The values of T_0 , depending on the considered initial dye concentrations, are presented in Table V. Their values showed that the adsorption process was spontaneous above the standard free-energy temperature and nonspontaneous below this value, with an adsorption capacity that was greater at $T > T_0$ because of the greater decrease in the free energy at the adsorbate-adsorbent surface.³⁹

Characterization of the Cation-Exchange Resins

In accordance with other literature information,^{17,19,27,41} the structural characterization of the ion-exchange resins before and after BB9 dye adsorption was performed by FTIR spectroscopy and ESEM analysis.

The FTIR spectra of the C145 resins [Figure 5(a)] showed characteristic absorption of the aromatic ring in the area $3100\text{--}300 \text{ cm}^{-1}$. Two strong bands observed at 2926 and 2854 cm^{-1} were assigned to asymmetric C—H and symmetric C—H bands,

respectively. Other characteristic absorptions were observed at 1240 and 1130 cm^{-1} ; these were attributed to —SO_3^- asymmetric and symmetric stretching, respectively. After BB9 dye adsorption, some small shifts were observed as an indication of the bonding interaction between SO_3^- and the aromatic ring of BB9 dye.⁴² Other authors emphasized the bond formation between the SO_3^- and nitrogen of the aromatic ring of BB9.⁴³

The analyzed C107E sample shows in the FTIR absorptions characteristics, namely, a broad bonded O—H stretching vibration in the region $3700\text{--}3100 \text{ cm}^{-1}$, which was characteristic of carboxylic groups. The stretching absorption band at 1720 cm^{-1} was assigned to the C=O bond in carboxylic groups. The adsorbed BB9 dye onto the microbead copolymer led to significant changes in the FTIR spectra [see Figure 5(b)]. The changes occurred mainly in the OH ($3700\text{--}3100 \text{ cm}^{-1}$) and CH ($2959\text{--}2855 \text{ cm}^{-1}$) region, and also, a new absorption band due to BB9 was observed at 1639 cm^{-1} . All of these changes were a clear indication of interactions that took place between BB9 and the C107E resin.

The surface morphology of both ion-exchange resins before and after the adsorption of BB9 dye was emphasized by ESEM and is shown in Figure 6.

The microbeads of both C107E and C145 had regular spherical shapes, with a compact structure within the size range of $400\text{--}800 \mu\text{m}$ [Figure 6(a,b,d,e)]. The pore size distribution of C107E and C145 showed an almost exclusive macroporosity with very little microporous structure ($<5\%$). However, the pore size of C145 was in the range $80\text{--}150 \text{ nm}$, whereas for C107E, the pore size was situated in the range $250\text{--}500 \text{ nm}$. These findings correlated well with published values of the surface area (determined by N_2 adsorption and the application of Brunauer-Emmett-Teller theory) and were $20 \text{ m}^2/\text{g}$ for C145 and a few hundred square meters per gram for C107E.⁴⁴

Because of their specific surface characteristics, the BB9 dye adsorption onto the microbeads was emphasized by ESEM; C107E, because of its porous structure, allowed the BB9 dye to migrate inside the microsphere structure. After this process, the surface had a swollenlike structure. Conversely, the C145 microbeads did not easily allow a diffusion process of the BB9 dye; this was clearly visible on the microsphere's surface (Figure 6).

These aspects could be explained when we took into account the likely behavior of the dye in strongly alkaline medium, the structure of the polymer matrix resins (polystyrene and polymethacrylate, respectively, reticulated with divinylbenzene), and the nature of the functional groups ($\text{—SO}_3^- \text{Na}^+$ and $\text{—COO}^- \text{H}^+$, respectively) of the resins that had different possibilities of dissociation in basic medium. Thus, basic medium could produce an aggregation of dye molecules, which was detrimental to the adsorption process. Also, the aggregates of dye could penetrate with great difficulty or not within the microbeads of the resin. In the case of the C145 resin, the polymer matrix structure allowed the retention of these aggregates on the BB9 particle surface [Figure 6(f)]; this did not seem possible in the case of the C107E resin [Figure 6(c)].

Desorption and Regeneration Studies

To elucidate the nature of the adsorption of BB9 dye onto the PuroLite cation-exchange resins, desorption studies were

performed in accordance with literature data.^{12,13,17,45} The obtained results are shown in Table VI.

The obtained results indicate that sulfuric acid was a better reagent for desorption because more than 85% of the adsorbed dye was removed. BB9 desorption by mineral acids indicated that the dye was adsorbed onto both resins through by an ion-exchange mechanism. The increasing temperature and the increasing shaking time of the phases had a favorable effect on the desorption of BB9 dye from the resins. The presence of an organic solvent, namely, methanol, in an aqueous solution of hydrochloric acid improved the dye desorption performance. The effect was more important in case of the sulfonic resin; this confirmed the presence of hydrophobic interactions between the adsorbed dye molecules and the aromatic matrix of the resin.

After regeneration, colorless resins beads were obtained, and more than five adsorption–desorption cycles were performed without a significant decrease in the adsorption capacity of both resins for BB9 dye.

CONCLUSIONS

In this study, we focused on evaluating the adsorptive potential of two types of Purolite resins (C145, a strongly acidic cation exchanger, and C107E, a weakly acidic cation exchanger) for the removal of BB9 dye from aqueous solutions. The obtained results led us to the following conclusions:

- The adsorption of BB9 dye onto C145 and C107E, strongly and weakly acidic, respectively, Purolite cation-exchange resins depended on the physicochemical characteristics of the resins, the amount of adsorbent, the initial dye concentration, the pH value, the temperature, and the phase contact time.
- The equilibrium adsorption data analyzed by the Freundlich, Langmuir, and DR isotherm models confirmed that the Freundlich model described the equilibrium data for both resins well. The obtained monolayer adsorption capacities ranged from 29.154 to 54.645 mg/g (C145) and 28.248 to 54.054 mg/g (C107E), when the initial dye concentration was varied between 12.8 and 260 mg/L at 20°C, pH 10, and a 5-h phase contact time.
- The adsorption capacities of the studied resins increased with increasing temperature from 5 to 50°C; this suggested an endothermic nature of adsorption process, information that was also confirmed by the values of the thermodynamic parameters.
- The physicochemical analyses (FTIR spectroscopy and ESEM) confirmed that the BB9 dye adsorption on the studied cationic resins mainly arose through an ion-exchange mechanism.
- All these results highlight the ability of these cation exchangers to bind the BB9 dye from aqueous medium; this could be useful in the retention of dye from industrial effluents before discharge into municipal collection tanks.
- At the same time, the results offer valuable information for further research on the kinetics of the process to determine the rate-limiting step and to assess the mechanisms of the adsorption and desorption processes.

- Desorption experiments carried out by the batch method with desorption reagents solutions of 0.1–1 mol/L HCl, 2.5 mol/L H₂SO₄, CH₃OH, and a mixture of 1 mol/L HCl and CH₃OH confirmed that the BB9 dye adsorption process was achieved by an ion-exchange mechanism complemented by hydrophobic interactions. The use of the sulfuric acid desorption reagent was found to be most effective because more than 85% of the adsorbed dye was removed.

REFERENCES

1. Zaharia, C.; Suteu, D. In *Organic Pollutants Ten Years After the Stockholm Convention—Environmental and Analytical Update*; Puzyn, T., Mostrag-Szlichtyng, A., Eds.; INTECH: Rijeka, Croatia, **2012**; Chapter 3, p 57.
2. Latif, A.; Noor, S.; Sharif, Q. M.; Najeebullah, M. *J. Chem. Soc. Pak.* **2010**, *32*, 115.
3. Zaharia, C.; Suteu, D.; Muresan, A. *Environ. Eng. Manage. J.* **2012**, *11*, 493.
4. Ramesh Babu, B.; Parande, A. K.; Raghu, S.; Prem Kumar, T. *J. Cotton Sci.* **2007**, *11*, 141.
5. Zaharia, C.; Suteu, D.; Muresan, A.; Muresan, R.; Popescu, A. *Environ. Eng. Manage. J.* **2009**, *8*, 1359.
6. Greluk, M.; Hubicki, Z. *Chem. Eng. J.* **2011**, *170*, 184.
7. Wawrzkiwicz, M.; Hubicki, Z. *J. Hazard. Mater.* **2009**, *164*, 502.
8. Greluk, M.; Hubicki, Z. *Chem. Eng. J.* **2010**, *162*, 919.
9. Wawrzkiwicz, M.; Hubicki, Z. *J. Hazard. Mater.* **2009**, *172*, 868.
10. Wawrzkiwicz, M.; Hubicki, Z. *Chem. Eng. J.* **2010**, *157*, 29.
11. Suteu, D.; Bilba, D.; Zaharia, C. *Hung. J. Chem.* **2002**, *30*, 7.
12. Bayramoglu, G.; Altintas, B.; Yakup Arica, M. *Chem. Eng. J.* **2009**, *152*, 339.
13. Dulman, V.; Simion, C.; Barsanescu, A.; Bunia, I.; Neagu, V. *J. Appl. Polym. Sci.* **2009**, *113*, 615.
14. Wawrzkiwicz, M.; Hubicki, Z. *Environ. Technol.* **2009**, *30*, 1059.
15. Wawrzkiwicz, M.; Hubicki, Z. *Cent. Eur. J. Chem.* **2011**, *9*, 867.
16. Wawrzkiwicz, M.; Hubicki, Z. *Sep. Sci. Technol.* **2010**, *45*, 1076.
17. Yavuz, E.; Bayramoglu, G.; Aricab, M. Y.; Senkala, B. F. *J. Chem. Technol. Biotechnol.* **2011**, *86*, 699.
18. Suteu, D.; Bilba, D.; Dan, F. *J. Appl. Polym. Sci.* **2007**, *105*, 1833.
19. Crini, G. *Bioresour. Technol.* **2006**, *97*, 1061.
20. Suteu, D.; Bilba, D. *Acta. Chim. Slov.* **2005**, *52*, 73.
21. Gupta, V. K.; Carrott, P. J. M.; Ribeiro, M. M. L.; Suhas. *Crit. Rev. Environ. Sci. Technol.* **2009**, *39*, 783.
22. Demirbas, A. *J. Hazard. Mater.* **2009**, *167*, 1.
23. Rafatullah, M.; Sulaiman, O.; Hashim, R.; Ahmad, A. *J. Hazard. Mater.* **2010**, *177*, 70.

24. Ahmaruzzaman, M. *Prog. Energy Combust. Sci.* **2007**, *36*, 327.
25. Suteu, D.; Zaharia, C.; Muresan, A.; Muresan, R.; Popescu, A. *Environ. Eng. Manage. J.* **2009**, *8*, 1097.
26. Macoveanu, M.; Bilba, D.; Bilba, N.; Gavrilescu, M.; Soreanu, G. Ion Exchange Process in Environmental Protection (in Romanian); MatrixRom: Bucharest, **2002**.
27. Karcher, S.; Kornmuller, A.; Jekel, M. *Water Res.* **2002**, *36*, 4717.
28. Yu, Y.; Zhuang, Y.-Y.; Wang, Z.-H.; Qiu, M.-Q. *Chemosphere* **2004**, *54*, 425.
29. Gut, F.; Schiek, W.; Haefeli, W. E.; Walter-Sack, I.; Burhenne, J. *Eur. J. Pharm. Biopharm.* **2008**, *69*, 682.
30. Rehman, R.; Anwar, J.; Mahmud, T. *J. Chem. Soc. Pak.* **2012**, *34*, 460.
31. Ho, Y. S. *Carbon* **2004**, *42*, 2113.
32. Tsai, S. C.; Juang, K. W. *J. Radioanal. Nucl. Chem.* **2000**, *243*, 741.
33. Tanaka, H.; Nakagawa, T.; Okabayashi, Y.; Aoyama, H.; Tanaka, T.; Itho, K.; Chikuma, M.; Saito, Y.; Sakurai, H.; Nakayama, M. *Pure Appl. Chem.* **1987**, *59*, 573.
34. Mills, A.; Hazafy, D.; Parkinson, J.; Tuttle, T.; Hutchings, M. G. *Dyes Pigments* **2011**, *88*, 149.
35. Ozdenir, F. A.; Demirata, B.; Apak, T. *J. Appl. Polym. Sci.* **2009**, *112*, 3442.
36. Noor, E.; Al-Solmi, F. M. E.-J. *Chemistry* **2011**, *8*, S171.
37. Crini, G.; Badot, P. M. *Prog. Polym. Sci.* **2008**, *33*, 399.
38. Crini, G. *Dyes Pigments* **2008**, *77*, 415.
39. Doke, K. M.; Khan, E. M. *Rev. Environ. Sci. Biotechnol.*, DOI 10.1007/s11157-012-9273-z.
40. Abd El-Latif, M. M.; Ibrahim, A. M.; El-Kady, M. F. *J. Am. Sci.* **2012**, *6*, 267.
41. Muntean, S. G.; Paska, O.; Coseri, S.; Simu, G. M.; Grad, M. E.; Ilia, G. *J. Appl. Polym. Sci.*, **2013**, *127*(6), 4409.
42. Rezaei-Zarchi, S.; Javed, A.; Mirjalili, H.; Bari Abarghouei, H.; Ali Hashemizadeh, S. *Turk. J. Chem.* **2009**, *33*, 411.
43. Watanabe, A.; Fujitsuka, M.; Ito, O. *Thin Solid Films* **1999**, *354*, 13.
44. Jones, M. D. (to British Petroleum Co.). Eur. Pat. 0484020 (1996).
45. Karcher, S.; Kornmuller, A.; Jekel, M. *Water Res.* **2002**, *36*, 4717.